

8×10^{-17} fractional laser frequency instability with a long room-temperature cavity

Sebastian Häfner,¹ Stephan Falke,^{1,*} Christian Grebing,¹ Stefan Vogt,¹
Thomas Legero,¹ Mikko Merimaa,² Christian Lisdat,¹ and Uwe Sterr¹

¹*Physikalisch-Technische Bundesanstalt (PTB), Bundesallee 100, 38116 Braunschweig, Germany*

²*VTT Technical Research Centre of Finland Ltd Centre for Metrology MIKES, P.O. Box 1000, FI-02044 VTT, Finland*

compiled: April 1, 2015

We present a laser system based on a 48 cm long optical glass resonator. The large size requires a sophisticated thermal control and optimized mounting design. A self balancing mounting was essential to reliably reach sensitivities to acceleration of below $\Delta\nu/\nu < 2 \times 10^{-10}$ /g in all directions. Furthermore, fiber noise cancellations from a common reference point near the laser diode to the cavity mirror and to additional user points (Sr clock and frequency comb) are implemented. Through comparison to other cavity-stabilized lasers and to a strontium lattice clock an instability of below 1×10^{-16} at averaging times from 1 s to 1000 s is revealed.

OCIS codes: 140.4780, 140.3425, 120.3940
<http://dx.doi.org/10.1364/XX.99.099999>

Lasers with high frequency stability are urgently needed in various fields of physics and technology, e.g. for precision measurements, for operation of optical clocks [1, 2] or generation of low phase noise microwave signals [3]. The stability of today's best optical clocks [4] is limited by laser frequency noise due to the Dick effect [5]. While alternative concepts for laser frequency stabilization like spectral hole-burning [6], or active atomic clocks [7] are currently under investigation, most ultra-stable lasers are based on well isolated resonators. The best present room-temperature resonators provide fractional laser instabilities of $1\text{--}2 \times 10^{-16}$ [8, 9], limited by the thermal Brownian noise from their constituents [10], with the biggest contributions from mirror coatings. This noise can be reduced by operation at cryogenic temperatures [11], increasing the mode size [12], or using a longer cavity [9].

Here we employ the latter approach and report on the design and evaluation of a 48 cm long room temperature resonator with a spacer made from ultra-low expansion glass (ULE). Compared to a cryogenic cavity, we can operate the system at ambient temperatures directly at the Sr lattice clock 698 nm transition [13], which simplifies the system and its operation. However, the use of long cylindrical and heavier cavities makes it much more difficult to reach the required suppression of optical length changes through forces induced by seismic vibrations and through thermal expansion caused by

temperature fluctuations. In the following, we describe the vibration insensitive mounting, temperature control, optical setup and fiber noise cancellation system.

We use a cylindrical ULE-glass spacer of 48 cm length and 9 cm diameter. With two optically contacted fused silica mirrors (plane and radius of curvature $R = 1$ m) we expect a thermal noise level [14] of 5.4×10^{-17} . The system provides a cavity finesse $F = 282\,000$ (1.1 kHz linewidth) as measured from optical ring down. Before the final optical contact, the finesse was optimized by moving the mirrors to minimize the influence of coating defects. ULE rings are attached to the rear sides of both mirrors to avoid the effect of the differential thermal expansion between the fused silica substrate and the ULE glass spacer [15]. The resonator is held horizontally on four points (Fig. 1) in small cutouts (length 40 mm, depth 4 mm) machined to the sides of the spacer [16–18]. Accelerations acting on the resonator due to seismic noise both change the cavity length L_{geo} between the nominal centers of the mirrors (geometrical axis) and lead to tilts of the mirrors through bending of the spacer. Mirror tilt leads to a change in the optical length if there is a mismatch between the geometrical axis and the optical axis. The high symmetry of the resonator and mount largely suppresses the sensitivity of L_{geo} to accelerations in y and z directions. In addition positions and dimensions of the cutouts were optimized by Finite Element Modeling (FEM) to minimize bending and the sensitivity along x . For a long and heavy spacer ($m = 6.8$ kg) as used here, the symmetry of the reaction forces along the optical axis (z) as well in the transverse horizontal direction (y) becomes more important, as already a force

* Current address: TOPTICA Photonics AG, Lochhamer Schlag 19, 82166 Gräfelfing

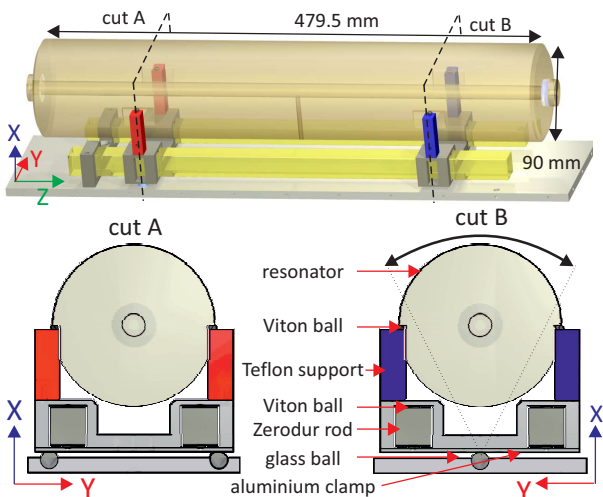


Fig. 1. Resonator mounting design. The lower figures show cuts through the fixed (A) and rotatable (B) support.

difference of 100 nN between the mounting points (along z) leads to a relative length change of 1.3×10^{-16} . Assuming a typical vibration noise of $1 \mu\text{g}$, these reaction forces need to be balanced on a level of 10^{-3} to reach a fractional instability below 10^{-16} . The elasticity at all four mounting positions has to be matched very accurately in order to obtain this level of balance of forces.

In our design the cavity is sitting on four Viton balls (diameter 4 mm), which are placed on top of four Teflon posts. Through height imperfections of the posts, the Viton pieces get compressed differently and the shearing elasticity differs. Thus, the requirements given above are violated. To remove the height imperfections and realize an effective three point mount, a self balancing mount is employed (Fig. 1). Near one end of the resonator (cut B), the two Teflon posts supporting the resonator are mounted on an aluminum clamp on top of a single glass sphere, allowing the structure to rotate around the z -axis. On the other end (cut A) rotation of the structure around the z -axis is prevented by two glass spheres underneath the clamp. Thus, the four posts is automatically leveled and the forces at the support points are equalized by this movement of the whole cavity.

To isolate the mounting structure from the thermal expansion of the aluminum base plate, two Zerodur glass rods are inserted between the clamp and the base plate (Fig. 1). Viton balls between the clamps and the glass rods ensure a strong friction force to prevent a horizontal movement of the clamps while providing the necessary flexibility for the balanced mount. By experimentally varying the distance between the Viton balls that hold the resonator, the vibration sensitivities κ_i were optimized to $\kappa_z = 1.7 \times 10^{-10} / \text{g}$, $\kappa_y = 0.5 \times 10^{-10} / \text{g}$ and $\kappa_x = 1.5 \times 10^{-10} / \text{g}$; all measured at 0.7 Hz, in contrast to poorly reproducible values around $4 \times 10^{-8} / \text{g}$ which were initially obtained without balanced mount.

We measured the thermal expansion coefficient α of

the resonator as $\alpha(T) = 2 \times 10^{-9} \text{ K}^{-2}(T - T_0)$ with a zero-crossing temperature of $T_0 = -0.24 \text{ }^\circ\text{C}$. Thus, if operated within 50 mK of T_0 , a temperature stability of better than $1 \mu\text{K}$ is required to reach a fractional frequency instability of below 10^{-16} . The large dimensions of the setup can easily lead to large temperature gradients that fluctuate with the ambient temperature, which exacerbates the control of the average temperature of the resonator at the required level. To achieve the required stability we start by stabilizing the temperature of the vacuum chamber by thermoelectric coolers (TEC) close to ambient temperature.

Inside the vacuum chamber, the temperature of the first heat shield is stabilized at T_0 using TECs mounted between the shield and the chamber. To reduce the influence of thermal gradients on the cavity, this first shield is temperature stabilized in three sections along the axial direction (z). For each section a weighted temperature from thermistors at the top and bottom ($\approx 1 : 5$) of the shield is used as input to a temperature control loop. The relative contributions of the sensors were determined experimentally by introducing gradients in the vacuum chamber and minimizing the remaining temperature fluctuation of the second shield. Further inside, a third heat shield surrounds the resonator. The polished aluminum heat shields act as low pass filter for temperature fluctuations with a measured time constant of $\tau_{\text{th}} \approx 8 \text{ d}$. With this advanced temperature control,

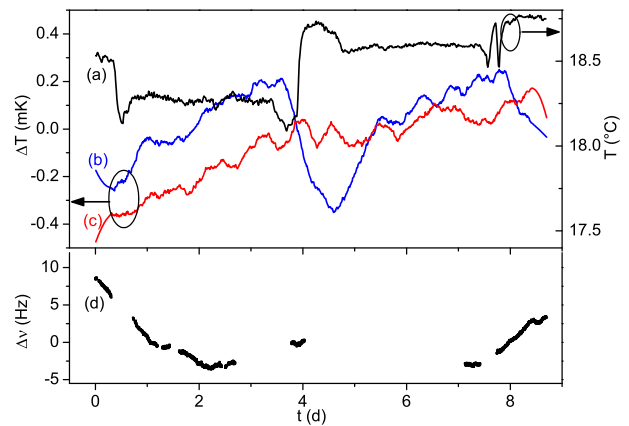


Fig. 2. Temperature in the acoustic isolation box surrounding the vacuum chamber (a), temperature fluctuation on the active heat shield (b) and next to the cavity (c). (d) shows residual cavity frequency fluctuations measured against the Sr reference with a linear drift of 20 mHz/s subtracted.

the temperature fluctuations of the outer passive shield remain within $\approx 500 \mu\text{K}$ when the room temperature changes by 0.5 K (Fig. 2). At the resonator no significant influence was observed. After removal of an average drift of 20 mHz/s due to aging of the spacer material, the frequency of the resonator fluctuates by $\pm 6 \text{ Hz}$. Assuming an offset of the resonator temperature from T_0 of 50 mK, these frequency deviations correspond to temperature fluctuations of $\pm 120 \mu\text{K}$.

This resonator setup is the central part of the interrogation laser system for a ^{87}Sr optical lattice clock [13]. The frequency of a filter-stabilized 698 nm extended-cavity laser diode [19, 20] is locked via the Pound-Drever-Hall (PDH) technique to the cavity [21]. The light is sent through an offset-AOM, which allows tuning the frequency to the ^{87}Sr clock transition, and via a 2 m long optical fiber to the vibration isolation table. There, the light is phase modulated by a free space electro-optic modulator (EOM) required for PDH-stabilization and then sent through several windows to the resonator. Any reflection from optical components in the optical path back to the cavity leads to frequency pulling of the cavity resonance. By placing a quarter wave plate inside the vacuum system directly in front of the cavity mirror, all these reflections have orthogonal polarization with respect to the initial polarization and should not contribute to frequency pulling.

Faraday isolators, 35 dB before and 38 dB behind the EOM suppress effects of spurious reflections, which may also produce residual amplitude modulation (RAM). The potential frequency shift due to RAM is on the order of 10^{-17} , thus no active control was implemented. Significant frequency shifts are introduced by thermal deformation and optical length change caused by light absorbed in the mirror coatings. It leads to a sensitivity of 120 Hz per μW of power transmitted through the cavity. We send a power of 35 μW to the resonator about 70% of the carrier is coupled in and 2 μW are transmitted. The transmitted power was stabilized with the offset-AOM. An out-of-loop measurement of the power stability converts into a frequency instability below 5×10^{-17} at 1 s averaging time. The calculated instability from the shot noise for both the transmitted as well as the light for the PDH lock is well below 10^{-17} .

The optical path lengths (including optical fibers) to the reference cavity, to the Sr experiment, and to a frequency comb are all stabilized, using a common reference mirror near the clock laser. Special attention is paid to the optical path between the reference mirror and the cavity. Since it is inside the PDH-stabilization loop, any phase noise ϕ_{path} from length fluctuations is added to the laser light at the reference mirror and to the light sent elsewhere. A path length stabilization by retro-reflecting light from the cavity back through the fiber [22] is incompatible with the required optical isolation as described above. To circumvent this dilemma, we deliver phase-stable light with an additional noise canceled fiber using the common reference mirror and superimpose it with the light transmitted through the reference cavity. Phase fluctuations in the heterodyne beat signal originate from ϕ_{path} and are compensated through the offset-AOM.

The system performance was evaluated by comparison to a laser locked to a cryogenic silicon cavity at 1542 nm [11] via a frequency comb and a 698 nm transportable laser system based on a 12 cm long ULE-cavity with fused silica mirrors. From the simultaneously sam-

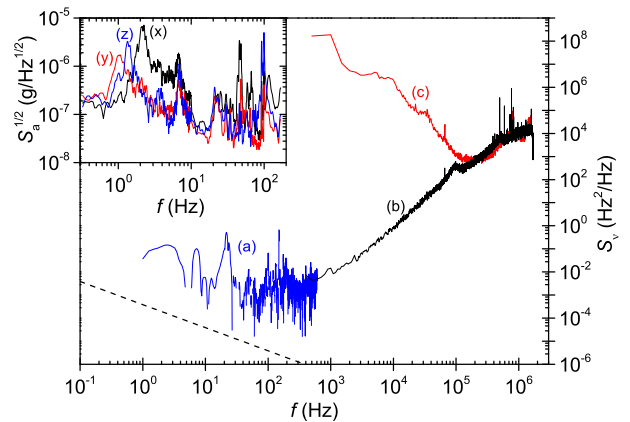


Fig. 3. Noise spectrum of the laser locked to the cavity from a three cornered hat method in the frequency domain (a), from the light transmitted through the cavity (b), of the free running laser (c) and calculated cavity thermal noise (dashed black line). For details see text. The inset displays the power spectral density of acceleration S_a on the passive vibration isolation table close to the cavity, in x, y, z -direction.

pled two optical beats between these systems, the spectral power densities of frequency fluctuations $S_y(f)$ between all three systems were calculated. As these statistical spectral quantities behave the same way as Allan variances σ_y^2 , the individual noise components $S_v(f)$ were computed with the three-cornered hat method [23] (Fig. 3a). For higher Fourier frequencies, the noise was estimated from the beat between the spectrally filtered light transmitted through the cavity with light coming directly from the laser (b). At high frequencies, this noise approaches the frequency noise of the free running laser (c).

The inset in Fig. 3 shows the acceleration spectrum perturbing the cavity. Frequency features at 1 Hz and 7 Hz from resonances of the passive table can also be identified in the laser spectrum. The laser noise peak at 20 Hz, which is not clearly visible in the vibration spectra, presumably originates from a mechanical resonance of the resonator mounted on the Teflon posts.

The stability of the laser system for averaging times between 100 ms to 10 s was calculated with the three-cornered hat method with the two lasers mentioned above (Fig. 4). Frequency data were taken by three frequency counters over 10 h with a gate time of 100 ms and a single linear drift was subtracted. The data set was cut in over 100 sections and the individual Allan deviations were calculated.

The stability from 10 s to 2000 s was calculated by analyzing the offset frequency from the Sr transition shown in Fig. 2d. The data set of about 240 000 s was cut in 10 000 s long sections, a linear drift for each section was removed for compensating the temperature drift, and the Allan deviations were calculated. For both methods, the arithmetic mean of the deviations are shown in Fig. 4. The measured instability of 8×10^{-17} nearly

reaches the calculated thermal noise floor of 5.4×10^{-17} . The outstanding frequency stability of below 10^{-16} for averaging times from 1 s up to 1000 s indicates high seismic noise suppression and good thermal control. We assume that the stability at short averaging times is still limited by seismic noise and the free running laser linewidth in combination with the PDH servo bandwidth of 0.8 MHz.

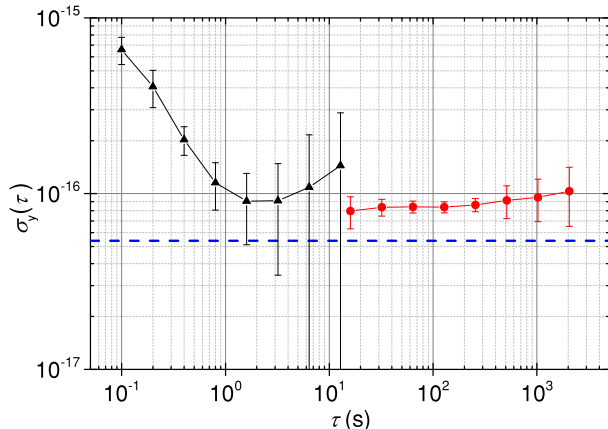


Fig. 4. Allan deviation (overlapping) of the cavity-stabilized laser system from three-cornered hat method (black triangles), and from comparison to the Sr reference (red circles) with linear drift removed. The dashed line indicates the calculated thermal noise level.

We have presented to our knowledge the first frequency stabilized laser setup that shows a stability below 1×10^{-16} over a wide range of averaging times, close to the thermal noise limit of this 48 cm long cavity. Both the observed flicker floor near the thermal limit and the deviations from a predictable linear drift are comparable to cryogenic ($T = 124$ K) single crystal silicon resonators [14, 24]. This was possible by implementing a novel vibration insensitive mount, temperature control, and optical path length control all the way to the cavity mirror. With laser systems like this, optical clocks will be improved by reducing the Dick effect and allowing Fourier limited linewidths for interrogation times beyond one second.

This work was supported by the Centre of Quantum Engineering and Space-Time Research (QUEST), the German Research Foundation (DFG) through the RTG 1729 ‘Fundamentals and Applications of ultra-cold Matter’ and the CRC 1128 geo-Q ‘Relativistic geodesy and gravimetry with quantum sensors’, the European Commission’s FP7 within SOC2 and the European Metrology Research Programme (EMRP) under QESOCAS and ITOC. The EMRP is jointly funded by the EMRP participating countries within EURAMET and the European Union.

We thank E. Rasel’s group at LUH for providing the laser and E. Tiemann’s group, from LUH, for providing the ULE glass spacer and also numerous people from PTB’s mechanical, electronic workshop for help and ad-

vice as well as Ch. Tamm for fruitful discussions.

References

- [1] T. Rosenband, D. B. Hume, P. O. Schmidt, C. W. Chou, A. Brusch, L. Lorini, W. H. Oskay, R. E. Drullinger, T. M. Fortier, J. E. Stalnaker, S. A. Diddams, W. C. Swann, N. R. Newbury, W. M. Itano, D. J. Wineland, and J. C. Bergquist, “Frequency ratio of Al^+ and Hg^+ single-ion optical clocks; metrology at the 17th decimal place,” *Science* **319**, 1808–1812 (2008).
- [2] I. Ushijima, M. Takamoto, M. Das, T. Ohkubo, and H. Katori, “Cryogenic optical lattice clocks,” *Nature Photonics* **9**, 185–189 (2015).
- [3] A. Bartels, S. A. Diddams, C. W. Oates, G. Wilpers, J. C. Bergquist, W. H. Oskay, and L. Hollberg, “Femtosecond-laser-based synthesis of ultrastable microwave signals from optical frequency references,” *Opt. Lett.* **30**, 667–669 (2005).
- [4] N. Hinkley, J. A. Sherman, N. B. Phillips, M. Schioppa, N. D. Lemke, K. Beloy, M. Pizzocaro, C. W. Oates, and A. D. Ludlow, “An atomic clock with 10^{-18} instability,” *Science* **341**, 1215–1218 (2013).
- [5] G. J. Dick, “Local oscillator induced instabilities in trapped ion frequency standards,” in “Proceedings of 19th Annu. Precise Time and Time Interval Meeting, Redondo Beach, 1987,” (U.S. Naval Observatory, Washington, DC, 1988), pp. 133–147.
- [6] M. J. Thorpe, L. Rippe, T. M. Fortier, M. S. Kirchner, and T. Rosenband, “Frequency-stabilization to 6×10^{-16} via spectral-hole burning,” *Nature Photonics* **5**, 688–693 (2011).
- [7] D. Meiser, J. Ye, D. R. Carlson, and M. J. Holland, “Prospects for a millihertz-linewidth laser,” *Phys. Rev. Lett.* **102**, 163601 (2009).
- [8] T. Nicholson, M. Martin, J. Williams, B. Bloom, M. Bishof, M. Swallows, S. Campbell, and J. Ye, “Comparison of two independent Sr optical clocks with 1×10^{-17} stability at 10^3 s,” *Phys. Rev. Lett.* **109**, 230801 (2012).
- [9] Y. Y. Jiang, A. D. Ludlow, N. D. Lemke, R. W. Fox, J. A. Sherman, L.-S. Ma, and C. W. Oates, “Making optical atomic clocks more stable with 10^{-16} level laser stabilization,” *Nature Photonics* **5**, 158–161 (2011).
- [10] K. Numata, A. Kemery, and J. Camp, “Thermal-noise limit in the frequency stabilization of lasers with rigid cavities,” *Phys. Rev. Lett.* **93**, 250602 (2004).
- [11] T. Kessler, C. Hagemann, C. Grebing, T. Legero, U. Sterr, F. Riehle, M. J. Martin, L. Chen, and J. Ye, “A sub-40-mHz-linewidth laser based on a silicon single-crystal optical cavity,” *Nature Photonics* **6**, 687–692 (2012).
- [12] S. Amairi, T. Legero, T. Kessler, U. Sterr, J. B. Wübbena, O. Mandel, and P. O. Schmidt, “Reducing the effect of thermal noise in optical cavities,” *Appl. Phys. B* **113**, 233–242 (2013).
- [13] S. Falke, N. Lemke, C. Grebing, B. Lipphardt, S. Weyers, V. Gerginov, N. Huntemann, C. Hagemann, A. Al-Masoudi, S. Häfner, S. Vogt, U. Sterr, and C. Lisdat, “A strontium lattice clock with 3×10^{-17} inaccuracy and its frequency,” *New J. Phys.* **16**, 073023 (2014).
- [14] T. Kessler, T. Legero, and U. Sterr, “Thermal noise in optical cavities revisited,” *J. Opt. Soc. Am. B* **29**, 178–184 (2012).

- [15] T. Legero, T. Kessler, and U. Sterr, “Tuning the thermal expansion properties of optical reference cavities with fused silica mirrors,” *J. Opt. Soc. Am. B* **27**, 914–919 (2010).
- [16] T. Nazarova, F. Riehle, and U. Sterr, “Vibration-insensitive reference cavity for an ultra-narrow-linewidth laser,” *Appl. Phys. B* **83**, 531–536 (2006).
- [17] S. A. Webster, M. Oxborrow, and P. Gill, “Vibration insensitive optical cavity,” *Phys. Rev. A* **75**, 011801(R) (2007).
- [18] J. Millo, D. V. Magalhães, C. Mandache, Y. Le Coq, E. M. L. English, P. G. Westergaard, J. Lodewyck, S. Bize, P. Lemonde, and G. Santarelli, “Ultrastable lasers based on vibration insensitive cavities,” *Phys. Rev. A* **79**, 053829 (2009).
- [19] X. Baillard, A. Gauguet, S. Bize, P. Lemonde, P. Laurent, A. Clairon, and P. Rosenbusch, “Interference-filter-stabilized external-cavity diode lasers,” *Opt. Commun.* **266**, 609–613 (2006).
- [20] M. Gilowski, C. Schubert, M. Zaiser, W. Herr, T. Wübbena, T. Wendrich, T. Müller, E. Rasel, and W. Ertmer, “Narrow bandwidth interference filter-stabilized diode laser systems for the manipulation of neutral atoms,” *Opt. Commun.* **280**, 443–447 (2007).
- [21] R. W. P. Drever, J. L. Hall, F. V. Kowalski, J. Hough, G. M. Ford, A. J. Munley, and H. Ward, “Laser phase and frequency stabilization using an optical resonator,” *Appl. Phys. B* **31**, 97–105 (1983).
- [22] L.-S. Ma, P. Jungner, J. Ye, and J. L. Hall, “Delivering the same optical frequency at two places: accurate cancellation of phase noise introduced by optical fiber or other time-varying path,” *Opt. Lett.* **19**, 1777–1779 (1994).
- [23] J. E. Gray and D. W. Allan, “A method for estimating the frequency stability of an individual oscillator,” in “Proc. 28th Frequency Control Symp., 29-31 May 1974, Atlantic City, New Jersey, New Jersey,” (Electronic Industries Association, 2001 Eye Street, N.W., Washington, D.C. 20006, 1974), pp. 243–246.
- [24] C. Hagemann, C. Grebing, C. Lisdat, S. Falke, T. Legero, U. Sterr, F. Riehle, M. J. Martin, and J. Ye, “Ultrastable laser with average fractional frequency drift rate below $5 \times 10^{-19}/s$,” *Opt. Lett.* **39**, 5102–5105 (2014).